LOW-RANK AND SPARSE MATRIX DECOMPOSITION WITH ORTHOGONAL COMPLEMENT SUBSPACE PROJECTION FOR HYPERSPECTRAL ANOMALY DETECTION

Xing Wu (1) (2), Xia Zhang (1)

[1] Institute of Remote Sensing and Digital Earth, Chinese Academy of Sciences, Beijing, 100101, China
[2] University of Chinese Academy of Sciences, Beijing, 100049, China
Email: wuxing@radi.ac.cn; zhangxia@radi.ac.cn

KEY WORDS: Hyperspectral Imagery, Anomaly Detection, Low-Rank and Sparse, Orthogonal Complement Subspace Projection

ABSTRACT: Anomaly detection is an active field in the hyperspectral imagery (HSI) processing, which distinguishes anomaly targets from complex backgrounds without a priori information. Recently, the low-rank and sparse matrix decomposition (LRaSMD) technique, which assumes the backgrounds are low-rank and the anomalies are sparse, was employed in hyperspectral anomaly detection and achieved competitive performance. In practice, some sporadic background pixels are divided into the sparse part. Thus, the LRaSMD method could encounter false alarms because it merely depends on the sparse term. To alleviate this problem, we propose a matrix decomposition-based orthogonal complement subspace projection algorithm (MDOCSP). Specifically, the preliminary sparse and low-rank parts of HSI were extracted by LRaSMD. Then a band-wise ratio was implemented between the anomaly and background to suppress the sporadic background pixels. Moreover, we projected the enhanced anomaly onto the orthogonal complement subspace of background to further reduce the false alarms. The proposed method was compared with five detectors, including Reed-Xiaoli (RX) detector, subspace RX (SSRX), cluster-based anomaly detector (CBAD), collaborative representation detector (CRD), LRaSMD and LRaSMD-based Mahalanobis distance (LSMAD) on a benchmark dataset. Corresponding to each competitor, it has the detection performance improvement of 10.66%, 21.29%, 3.9%, 3.41%, 0.49%, and 6.19%, respectively. Experiments demonstrated that MDOCSP outperforms several state-of-the-art detectors.

1. INTRODUCTION

Recent advances in hyperspectral remote sensor technology allow the simultaneous acquisition of hundreds of narrow spectral bands over a wide range of the electromagnetic spectrum [1-3]. Therefore, small and low probability objects can be accurately extracted by virtue of the high spectral resolution [4]. Target detection is a binary classifier to label every pixel in the image as a target or background. According to the availability of a priori knowledge of the target spectrum, target detection can be grouped into two categories: supervised and unsupervised [5]. Unsupervised target detection, also known as anomaly detection (AD) has drawn much attention due to no prior information of the target spectra is needed. AD has been widely used in various fields such as agriculture, geology, and ecology.

Numerous AD algorithms have been proposed for the past decades. Among them, the Reed-Xiaoli (RX) detector is considered as the benchmark of statistical based algorithm [6]. RX assumes the background follows a multivariate normal distribution and calculates the Mahalanobis distance between the pixel under test and the background. However, this assumption is unsuitable for describing a complicated and nonhomogeneous HSI. Several variations of the RX that attempt to alleviate the limitations have been proposed, such as subspace RX (SSRX) [7], cluster-based anomaly detector (CBAD) [8], random-selection-based anomaly detector (RSAD) [9], median-mean line (MML) RX [10]. To sidestep the difficulty of modeling the complicated distribution of background in statistics-based methods, the representation theory has been used in AD [11]. The collaborative representation detector (CRD) assumes the background pixels can be represented via a linear combination of surrounding samples generated by a dual window, while anomalies cannot [12]. Local sparsity divergence based detector exploits the fact that anomaly and background lie in different subspaces and anomaly cannot be effectively represented by its local neighbors, thus leading to different sparsity divergence [13].

The low-rank and sparse matrix decomposition technique has been successfully applied in AD [4, 14-16], which exploits the fact that the background spectra usually have high correlations and the anomalies are small and sparse objects. Low-rank and sparse matrix decomposition based detector (LRaSMD) [4] converts the HSI cube to a matrix and then decomposed the matrix as the sum of a low-rank part, a sparse part and a noise part by Go Decomposition (GoDec) algorithm [17]. The pixels with large L2 norm of the anomaly term are selected as anomalies. In [16], the authors pointed out some sporadic background pixels are incorrectly divided into the sparse part. Zhang, et al. [16] replaced the L2 norm in [4] with the Mahalanobis distance (labeled as LSMAD), which used the background component to suppress the contamination effect. Chang, et al. [15] further improved LSMAD by using a local Mahalanobis distance. However, the Mahalanobis distance works well when the data matches with the Gaussian assumption, which may not satisfy in reality.

Since the sparse part could not be the optimal anomaly of interest and it may contain some sporadic background materials, we propose a two-step improvement to alleviate the anomaly matrix contamination, namely matrix

decomposition-based orthogonal complement subspace projection algorithm (MDOCSP). The rest of this letter is organized as follows. Section 2 introduces related work and the proposed MDOCSP algorithm. The experimental results and analysis are presented in Section 3. Finally, the conclusions are drawn in Section 4.

2. METHODOLOGY

2.1 Related Work

Let $X=[x_1,x_2,\ldots x_N]^T$ be an HSI dataset, where $x_i \in R^{1\times B}$, N and B are the number of pixels and spectral channels. As the background spectra generally have high correlations, a potential low-rank structure may be present in it. The anomalies are often small in size or have a low probability of occurrence, thus anomaly matrix has a sparse property. Moreover, the dataset is often corrupted by an independent and identically distributed Gaussian noise. Therefore, the observed data X can be decomposed as the sum of the background matrix L, anomaly matrix S and noise matrix G

$$X = L + S + G \tag{1}$$

where $L \in R^{N\times B}$, $S \in R^{N\times B}$, $G \in R^{N\times B}$.

The equation (1) can be solved by minimizing the decomposition error with the rank and sparse constrains as follows:

$$\min_{L,S} \left\| X-L-S \right\|_F^2 \quad \text{s.t. } rank(L) \le r,\ card(S) \le kN \tag{2}$$

where $\left\|\cdot\right\|_F^2$ is the Frobenius norm, r and k denote the upper bound of the rank of L and the cardinality of S. The Go Decomposition (GoDec) algorithm is designed to solve the problem in model (2). It's an efficient and robust decomposition method, which uses the bilateral random projections to replace the time consuming singular value decomposition.

Once obtained the three decomposed components in equation (1), [4] directly utilized the Euclidean distance of sparse matrix S to calculate the anomaly value for each pixel

$$d_{ED}(x_i) = \sqrt{(S_{i,:}-\overline{S})(S_{i,:}-\overline{S})^T} \tag{3}$$

where $S_{i,:}$ is the anomaly component of spectral vector for pixel x_i, $\overline{S}$ is the mean row vector of the sparse matrix S. [16] further exploited the statistical features of background matrix to build a Mahalanobis distance based anomaly detector, which can mitigate the anomaly contamination problem in some extent. The detector can be formulated as follows:

$$d_{MD}(x_i) = (x_i-\mu_L)^T \Sigma_L^{-1} (x_i-\mu_L) \tag{4}$$

where μ_L and Σ_L are the mean and the covariance matrix of the low-rank background matrix L. A larger anomaly value indicates the pixel belongs to an anomaly with higher probability.

2.2 The Proposed Method

Different from the ordinary GoDec which imposes hard threshholding, Semi-Soft GoDec (SSGoDec) adopts soft thresholding to the entries of S. This change brings two key advantages: 1) the parameter k in constraint "$card(S) \le kN$" can be automatically determined by the soft-threshold r; 2) the time cost is substantially smaller than the ordinary GoDec. Here, we use SSGoDec to obtain the low-rank and sparse matrix. Since the sparse part could not be the optimal anomaly of interest and it may contain some sporadic background materials, we propose a two-step improvement to alleviate the anomaly matrix contamination. First, a band-wise ratio is calculated between the anomaly part and background part to suppress the sparse background pixels in the anomaly

$$A_{:,j} = S_{:,j} ./ L_{:,j},\ \ 1 \le j \le B \tag{5}$$

where $A_{:,j}$, $S_{:,j}$ and $L_{:,j}$ represent the j-th band of the ratio matrix, sparse matrix and background matrix, respectively. The operator $./$ denotes the element-wise division. Here A serves as the enhanced anomaly matrix.

As the anomaly and background lie in two orthogonal subspaces, we further exploit this fact by incorporating the background subspace information into the detector, which has a significant suppression on the contamination. We project the enhanced anomaly matrix onto the orthogonal complement subspace of background

$$Y_{i,:} = P_U^{\perp} A_{i,:} \tag{6}$$

$$P_U^{\perp} = I - U(U^T U)^{-1} U^T \tag{7}$$

where $P_U^{\perp}$ is the orthogonal complement subspace projector, U is the significant eigenvectors of covariance matrix of background, $I \in R^{B \times B}$ is an identity matrix, $Y_{i,:}$ denotes the projection result of pixel x_i. Once obtained $Y_{i,:}$, the anomaly value is determined by its ℓ_2-norm

$$d_{OCSP} = \left\| Y_{i,:} \right\| \quad 1 \le i \le N \tag{8}$$

The MDOCSP algorithm is depicted in Table 1.

Table 1. Pseudocode for MDOCSP

Algorithm 1: Pseudocode for MDOCSP

Input: a) The hyperspectral dataset X; b) the upper bound of the rank r, c) the Lagrange multiplier λ
Main:
1. Solve the optimization problem in model (2) using the SSGoDec algorithm.
2. Update the anomaly matrix A by Equation (5).
3. Implement the projector according to Equation (6).
4. Calculate the anomaly value for each pixel by ℓ_2-norm

Output: Anomaly detection map.

3. EXPERIMENTS

3.1 Datasets

The proposed algorithm is validated on one benchmark hyperspectral dataset, which was acquired by the Airborne Visible/Infrared Imaging Spectrometer (AVIRIS) from the San Diego airport area, CA, USA. It consists of 100×100 pixels and 224 bands at wavelengths ranging from 370 to 2510 nm. The spatial resolution is 3.5 m/pixel. After filtering out bands corresponding to water-absorption regions, low signal-to-noise ratio (SNR), and bad bands (1–6, 33–35, 97, 107–113, 153–166 and 221–224), 189 bands are retained. As shown in Fig. 1a, three airplanes in the upper right are anomalies, covering 58 pixels. Fig. 1b displays the ground truth.

(a) Image scene (b) Ground truth

Figure 1. AVIRIS dataset.

3.2 Experimental Results

The proposed algorithm was compared with the following detectors: RX [6], SSRX [7], CBAD [8], CRD [12], LRaSMD [4], and LSMAD [16]. For all algorithms except for RX, we chose the optimal parameters based on extensive experiments. All experiments were implemented using MATLAB 2018a on a desktop computer with a 3.4-GHz CPU and 16 GB of memory. The detection performance was evaluated by receiver operating characteristic (ROC) curve and area under the ROC curve (AUC) value.

A good detection ROC curve should lie near to the top left. For the AVIRIS dataset as shown in Fig. 4a, the ROC curve of MDOCSP is slightly above that of the LSMAD and LRaSMD detectors. All these three LRaSMD-based detectors outperform other state-of-the-art methods, demonstrating that LRaSMD technique is tenable in hyperspectral AD. The AUC value of each algorithm are shown in Table 2. The best AUC is displayed in bold. The proposed MDOCSP achieves the best detection performance among the competitors. The CBAD behaved better than RX and SSRX, but was inferior to CRD. The outstanding performance of MDOCSP over LRaSMD and LSMAD indicates: 1)

the significance of incorporating background information into detection decision; 2) the capability of OCSP to decrease the sporadic background pixels' interference. Figure 3 shows the detection maps of the different detectors. For visual interpretation, all the detection results are normalized to 0~1. As shown in Figure 3i, the responses of the isolated background pixels in the upper left are largely suppressed.

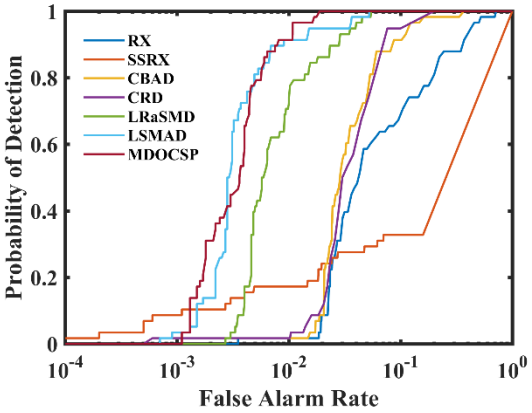

Figure 2. ROC curves of 7 detectors on AVIRIS dataset

Table 2. AUC values of different detectors

Methods	RX	SSRX	CBAD	CRD	LRaSMD	LSMAD	MDOCSP
AUC	0.8878	0.7428	0.9554	0.9603	0.9895	0.9325	**0.9944**

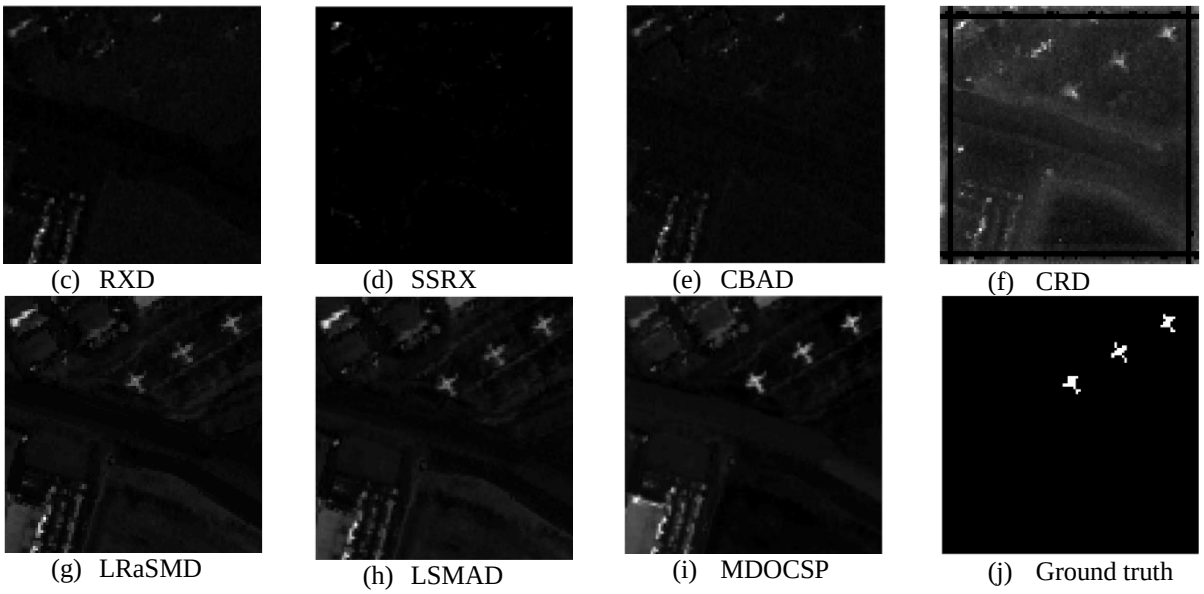

(c) RXD (d) SSRX (e) CBAD (f) CRD

(g) LRaSMD (h) LSMAD (i) MDOCSP (j) Ground truth

Figure 3. Detection maps for the AVIRIS dataset

We further analyzed the effect of the various parameters on detection performance of MDOCSP. Here, the range of λ is set as [1e-6, 1e-5, 1e-4, 1e-3, 0.05, 0.1], while the range of r is set from 1 to 10. Figure 4 illustrates the detection performance of MDOCSP versus the upper bound of the rank r and lagrange multiplier λ. The AUC values exceed 0.94 over a wide range of r and λ. A sudden decrease can be noticed when λ. exceeds 0.05, with the AUC value dropping to 0.77.

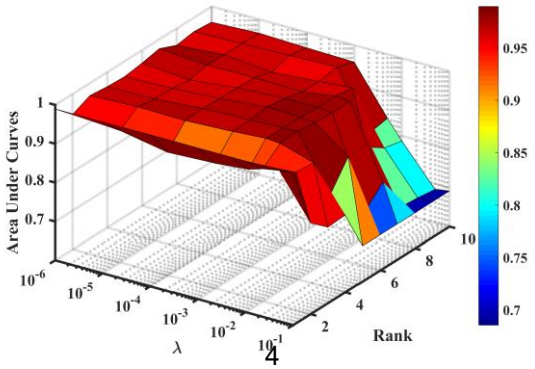

Figure 4. Detection performance of MDOCSP versus the upper bound of the rank r and lagrange multiplier λ.

4. CONCLUSION

In this work, we proposed a novel matrix decomposition-based orthogonal complement subspace projection algorithm (MDOCSP). Experiments on a benchmark dataset demonstrat that MDOCSP outperforms several state-of-the-art detectors. The effects of various parameters on detection performance are also investigated. Our future research will take the optimal parameters selection into consideration to promote detection performance.

5. ACKNOWLEDGMENT

This work was supported by National Natural Science Foundation of China (41671360).

6. REFERENCE

[1] A. Plaza *et al.*, "Recent advances in techniques for hyperspectral image processing," *Remote Sensing of Environment,* vol. 113, no. 1, pp. S110-S122, 2009.

[2] P. Ghamisi *et al.*, "Advances in Hyperspectral Image and Signal Processing: A Comprehensive Overview of the State of the Art," *IEEE Geoscience & Remote Sensing Magazine,* vol. 5, no. 4, pp. 37-78, 2018.

[3] N. M. Nasrabadi, "Hyperspectral Target Detection: An Overview of Current and Future Challenges," *IEEE Signal Processing Magazine,* vol. 31, no. 1, pp. 34-44, Jan 2014.

[4] W. W. Sun, C. Liu, J. L. Li, Y. M. Lai, and W. Y. Li, "Low-rank and sparse matrix decomposition-based anomaly detection for hyperspectral imagery," *Journal of Applied Remote Sensing,* vol. 8, May 2014, Art. no. 083641.

[5] Y. X. Yang, J. Q. Zhang, S. Z. Song, and D. L. Liu, "Hyperspectral Anomaly Detection via Dictionary Construction-Based Low-Rank Representation and Adaptive Weighting," *Remote Sensing,* vol. 11, no. 2, Jan 2019, Art. no. 192.

[6] I. S. Reed and X. L. Yu, "ADAPTIVE MULTIPLE-BAND CFAR DETECTION OF AN OPTICAL-PATTERN WITH UNKNOWN SPECTRAL DISTRIBUTION," *Ieee Transactions on Acoustics Speech and Signal Processing,* vol. 38, no. 10, pp. 1760-1770, Oct 1990.

[7] A. Schaum, "Joint subspace detection of hyperspectral targets," in *2004 IEEE Aerospace Conference Proceedings*, Big Sky, MT, 2004, vol. 3, pp. 1818-1824: IEEE.

[8] M. J. Carlotto, "A cluster-based approach for detecting man-made objects and changes in imagery," *IEEE Transactions on Geoscience and Remote Sensing,* vol. 43, no. 2, pp. 374-387, Feb 2005.

[9] B. Du and L. P. Zhang, "Random-Selection-Based Anomaly Detector for Hyperspectral Imagery," *IEEE Transactions on Geoscience and Remote Sensing,* vol. 49, no. 5, pp. 1578-1589, May 2011.

[10] M. Imani, "RX Anomaly Detector With Rectified Background," *IEEE Geoscience and Remote Sensing Letters,* vol. 14, no. 8, pp. 1313-1317, Aug 2017.

[11] W. Li and Q. Du, "A survey on representation-based classification and detection in hyperspectral remote sensing imagery," *Pattern Recognition Letters,* vol. 83, pp. 115-123, Nov 2016.

[12] W. Li and Q. Du, "Collaborative Representation for Hyperspectral Anomaly Detection," *IEEE Transactions on Geoscience & Remote Sensing,* vol. 53, no. 3, pp. 1463-1474, 2015.

[13] Z. Z. Yuan, H. Sun, K. F. Ji, Z. Y. Li, and H. X. Zou, "Local Sparsity Divergence for Hyperspectral Anomaly Detection," *IEEE Geoscience and Remote Sensing Letters,* vol. 11, no. 10, pp. 1697-1701, Oct 2014.

[14] L. X. Zhu, G. J. Wen, and S. H. Qiu, "Low-Rank and Sparse Matrix Decomposition with Cluster Weighting for Hyperspectral Anomaly Detection," *Remote Sensing,* vol. 10, no. 5, May 2018, Art. no. 707.

[15] H. W. Chang, T. Wang, A. H. Li, and H. Fang, "Local hyperspectral anomaly detection method based on low-rank and sparse matrix decomposition," *Journal of Applied Remote Sensing,* vol. 13, no. 2, Jun 2019, Art. no. 026513.

[16] Y. X. Zhang, B. Du, L. P. Zhang, and S. G. Wang, "A Low-Rank and Sparse Matrix Decomposition-Based Mahalanobis Distance Method for Hyperspectral Anomaly Detection," *Ieee Transactions on Geoscience and Remote Sensing,* vol. 54, no. 3, pp. 1376-1389, Mar 2016.

[17] T. Zhou and D. Tao, "Godec: Randomized low-rank & sparse matrix decomposition in noisy case," in *Proceedings of the 28th International Conference on Machine Learning, ICML 2011*, Bellevue,WA, 2011, pp. 33-40.